Reaction of Nitrogen Chelates with the $[Rh_2]^{4+}$ Core: Bis-Chelate Products and Demonstration of Reversible, Chelate-Based Reduction Processes

Charles A. Crawford,[†] John H. Matonic,[‡] John C. Huffman,[†] Kirsten Folting,[†] Kim R. Dunbar,*[,‡] and George Christou*[,†]

Department of Chemistry and Molecular Structure Center, Indiana University, Bloomington, Indiana 47405-4001, and Department of Chemistry, Michigan State University, East Lansing, Michigan 48824

Received August 22, 1996[⊗]

The preparations and properties are described of a series of $[Rh_2]^{4+}$ complexes possessing carboxylates and N-based chelates as ligands. Treatment of $Rh_2(O_2CR)_4(MeOH)_2$ (R = Me (**1**), Et (**2**), Ph (**3**) or CF_3 (**4**)) with 2 equiv of 2,2′-bipyridine (bpy) in refluxing MeCN leads to the $[Rh_2(O_2CR)_2(bpy)_2]^{2+}$ cation (in complexes **5**−**9**). Reaction of **1** with 1,10-phenanthroline (phen), 4,4′-dimethyl-2,2′-bipyridine (Me_2bpy), 4,4′-diphenyl-2,2′-bipyridine (Ph_2-bpy), and 4,7-diphenyl-1,10-phenanthroline (Ph_2phen) leads to the analogous cations of complexes **10**−**13**. Complex **6a**, $[Rh_2(OAc)_2(bpy)_2(MeCN)_2](PF_6)_2$·2MeCN, crystallizes in monoclinic space group $P2_1/a$ with the following cell parameters at −172 °C: a = 14.433(2) Å, b = 12.810(1) Å, c = 22.78(3) Å, β = 104.42(3)°, Z = 4, and V = 3971.2 Å^3. Complex **9**, $[Rh_2(O_2CCF_3)_4(bpy)_2]$·$Me_2CO$, crystallizes in triclinic space group $P\bar{1}$ with the following cell parameters at 20 °C: a = 14.260(4) Å, b = 15.375(4) Å, c = 9.709(2) Å, α = 105.98(2)°, β = 97.49(2)°, γ = 70.32(2)°, Z = 2, and V = 1925.2 Å^3. Both **6a** and **9** contain a singly-bonded $[Rh_2]^{4+}$ unit with two *cis* bridging RCO_2^- groups and two *syn*-bpy chelate groups in a near-eclipsed conformation about the Rh−Rh vector. Reaction of $[Rh_2(tpy)_2(MeCN)_4](BF_4)_4$ (**15**) (tpy = 2,2′:6′,2″-terpyridine) with $NBu^n_4(O_2CPh)$ gives $[Rh_2(O_2CPh)(tpy)_2(MeCN)_2](BF_4)_3$·MeCN (**16**). Complex **16** crystallizes in triclinic space group $P\bar{1}$ with the following cell parameters at −168 °C: a = 11.684(4) Å, b = 20.373(8) Å, c = 10.451(3) Å, α = 93.47(2)°, β = 110.53(1)°, γ = 100.03(2)°, Z = 2, and V = 2274.1 Å^3. The cation of **16** consists of a $[Rh_2]^{4+}$ unit with a bridging $PhCO_2^-$ group and two chelating tpy groups. The solution ^{1}H NMR properties of complexes **6**−**13** and **16** show the complexes to retain their solid-state structures on dissolution. The electrochemical properties of **6**−**13** and **16** were investigated by cyclic voltammetry (CV) and differential pulse voltammetry (DPV) in MeCN. The bis(bpy) and -(phen) complexes **6**−**8, 10**, and **11** show a reversible, one-electron reduction in the range −0.83 to −0.91 V *vs* ferrocene and an additional, irreversible reduction and an irreversible oxidation; the Ph_2bpy (**12**) and Ph_2phen (**13**) complexes show a two-electron reversible reduction at −0.61 to −0.76 and a reversible one-electron oxidation at 0.68−0.89 V. Consideration of the potentials as a function of carboxylate and chelate identity leads to the conclusion that the reductions are ligand (chelate)-based. This is supported by an extended Hückel calculation on the model compound $[Rh_2(O_2CH)_2(bpy)_2(HCN)_2]^{2+}$, which shows the LUMO to be a bpy-based orbital comprising in-phase, σ overlap of two bpy π^* orbitals, one on each of the *syn*-bpy groups. In contrast, complex **16** shows no reversible reduction processes. Complex **6b**, $[Rh_2(OAc)_2(bpy)_2(MeCN)_2](BF_4)_2$, in MeCN may be reduced with sodium acenaphthylenide in THF to give deep blue $[Rh_2(OAc)_2(bpy)_2(MeCN)_2](BF_4)$ (**14**) in high yield. The cation of **14** may also be generated by controlled potential electrolysis of **6a** in MeCN at −0.99 V and by heating of a solution of **6a** or **6b** in alcohol.

Introduction

Since the discovery of the first dinuclear rhodium(II) complex in 1960,[1] such compounds have been the focus of intensive research activity. Areas of interest include metal−metal bonding,[2] catalysis,[3] antitumor activity,[4] and coordination chemistry.[5] For a number of reasons, we have recently become interested in certain aspects of dinuclear Rh^{II} chemistry that encompass two of these areas, *viz*., coordination chemistry and antitumor activity. Thus, we are exploring the reactivity chemistry of the $[Rh_2]^{4+}$ core with nitrogen-based chelate ligands[6] and purine nucleobases,[7] aiming to achieve insight into the origin of the established antitumor activity of certain $[Rh_2]^{4+}$ complexes.[4]

Our initial investigations into the reactivity chemistry of the $[Rh_2]^{4+}$ core with N-based chelate ligands have demonstrated the ability of a single 2,2′-bipyridine (bpy) group to interact with the dimetal core in a variety of binding modes. These include axial−equatorial (ax−eq) and equatorial−equatorial (eq−eq) modes, and their characterization has provided valuable information concerning the mechanism by which the chelating ligand attaches to the $[Rh_2]^{4+}$ core.[6] With these results in hand,

[†] Indiana University.
[‡] Michigan State University.
[⊗] Abstract published in *Advance ACS Abstracts,* April 15, 1997.

(1) (a) Chernyaev, I. I.; Shenderetskaya, E. V.; Maiorova, A. G.; Karyagina, A. A. *Zh. Neorg. Khim.* **1960**, *5*, 1163. (b) Chernyaev, I. I.; Shenderetskaya, E. V.; Maiorova, A. G.; Karyagina, A. A. *Russ. J. Inorg. Chem. (Engl. Transl.)* **1960**, *5*, 559.

(2) (a) Casas, J. M.; Cayton, R. H.; Chisholm, M. H. *Inorg. Chem.* **1991**, *30*, 358. (b) O'Neill, F. M.; Boeyens, J. C. A. *Inorg. Chem.* **1990**, *29*, 1301. (c) Koh, Y. B.; Christoph, G. G. *Inorg. Chem.* **1978**, *17*, 2590. (d) Cotton, F. A.; DeBoer, B. G.; LaPrade, M. D.; Pipal, J. R.; Ucko, D. A. *Acta Crystallogr., Sect. B* **1971**, *27*, 1664. (e) Cotton, F. A. *Chem. Soc. Rev.* **1975**, *4*, 27. (f) Bennet, M. J.; Caulton, K. G.; Cotton, F. A. *Inorg. Chem.* **1969**, *8*, 1. (g) Cotton, F. A.; Norman, J. G. *J. Am. Chem. Soc.* **1971**, *93*, 80. (h) Cotton, F. A.; Walton, R. A. *Multiple Bonds Between Metal Atoms*; Wiley: New York, 1993; Chapter 7.

(3) (a) Felthouse, T. R. *Prog. Inorg. Chem.* **1982**, *29*, 73. (b) Boranovski, T. B. *Zh. Neorg. Khim.* **1982**, *27*, 1347. (c) Boyer, E. B.; Robinson, S. D. *Coord. Chem. Rev.* **1983**, *50*, 109. (d) Doyle, M. P. *Chem. Rev.* **1986**, *86*, 919. (e) Doyle, M. P. *Acc. Chem. Res.* **1986**, *19*, 348. (f) Pruchnik, F. P. *Pure Appl. Chem.* **1989**, *61*, 795.

S0020-1669(96)01028-2 CCC: $14.00

we have since sought to extend this chemistry to the reactions of $[Rh_2]^{4+}$ complexes with 2 equiv of a N-based chelate.

The first structurally-characterized $[Rh_2]^{4+}$ complex containing two chelating ligands was the dimethylglyoximate complex $Rh_2(OAc)_2(dmg)_2(PPh_3)_2$, which contains two bridging acetate ligands in a *cis* disposition about the dirhodium core.[8] The dimethylglyoximate ligands chelate in the four remaining equatorial positions, and the phosphine ligands are bound axially. Similar complexes are obtained with oxygen chelates such as β-diketonates.[9] In these systems, the chelates again occupy equatorial positions of the $[Rh_2]^{4+}$ core, and isomeric mixtures are obtained when asymmetry is present in the diketonate ligand.[10]

An additional group of compounds containing two nitrogen chelates bound to the $[Rh_2]^{4+}$ core are the $Rh_2(O_2CR)_2(N\text{-}N)_2X_2$ (R = H, Me, PhCH(OH); X = Cl, Br, I; N-N = bpy, phen) complexes.[3e,11] This chemistry was extended to the methyl-substituted phenanthroline (phen) derivatives and later to the cationic versions where the axial halide ligands are replaced with solvent molecules or neutral donors such as phosphines.[12] Reversible redox chemistry was observed with some of the species, and extended Hückel (EHT) calculations of the electronic structure of these complexes were performed[3e] in an attempt to compare them with the parent $Rh_2(O_2CR)_4L_2$ complexes. Calculations performed on the model compounds $Rh_2(O_2CH)_2(HN(CH)_2NH)_2X_2$ (X = Cl, Br) and $[Rh_2(O_2CH)_2(HN(CH)_2NH)_2L_2]^{2+}$ (L = H_2O, NH_3, PH_3, AsH_3) revealed a metal−metal bonding framework very similar to that found in the tetracarboxylate complexes, but concluded that the LUMO of the model complexes was largely ligand N−C π^* in character, but with significant contributions from the Rh−Rh π system.[3e]

In the present paper, we describe the syntheses of a number of complexes that contain two N-based chelate groups, together with single-crystal structural characterizations of three representative compounds. In addition, we describe and interpret the data obtained from application of a variety of spectroscopic and physicochemical techniques, supplemented with EHT calculations.

Experimental Section

Syntheses. All manipulations were performed under inert atmosphere conditions using standard Schlenk and glovebox techniques. $RhCl_3 \cdot 3H_2O$ (Sigma) was used as received. 2,2′-Bipyridine (bpy), 1,-10-phenanthroline (phen), 4,4′-dimethyl-2,2′-bipyridine (Me_2bpy), 4,4′-diphenyl-2,2′-bipyridine (Ph_2bpy), 4,7-diphenyl-1,10-phenanthroline (Ph_2phen), and 2,2′:6′,2″-terpyridine (tpy) were purchased from Aldrich Chemical Company and used as received. $Rh_2(O_2CMe)_4(MeOH)_2$ (**1**),[14] $Rh_2(O_2CR)_4(MeOH)_2$ (R = Et (**2**); R = Ph (**3**)),[15] $Rh_2(O_2CCF_3)_4(Me_2\text{-}CO)_2$ (**4**),[6b,14] and $[Rh_2(tpy)_2(MeCN)_4](BF_4)_4$ (**15**)[16] were prepared by literature procedures.

$[Rh_2(OAc)_2(bpy)_2](OAc)_2$ (5). A deep violet solution of **1** (200 mg, 0.377 mmol) in MeCN (12 mL) was treated with solid bpy (118 mg, 0.755 mmol). The mixture was heated to reflux for 24 h to give a brick red precipitate of **5**. The resulting solid was isolated by filtration and dried *in vacuo*. The yield was 284 mg, 83%. Anal. Calcd for $C_{28}H_{28}N_4O_8Rh_2$: C, 44.58; H, 3.74; N, 7.42. Found: C, 44.50; H, 3.64; N, 7.61. ^{1}H NMR in CD_3OD (ppm): O_2CCH_3, 1.900 (s, 6), 2.598 (s, 6); bpy, 7.44 (dt, 4) 7.95 (td, 4), 8.00 (d, 4), 8.38 (d, 4). Electronic spectrum in MeOH [λ_{max}/nm (ϵ_M/L mol^{-1} cm^{-1})]: 208 (25 000), 262 (30 000), 300 (15 170), 366 (3240), 432 (2080), 552 (300). IR data (KBr pellet, cm^{-1}): 3107 (w), 3079 (w), 2980 (w), 2926 (w), 1588 (s), 1563 (s), 1464 (m), 1451 (s), 1422 (s), 1364 (s), 1323 (m), 766 (m), 725 (w), 704 (m), 648 (w).

$[Rh_2(OAc)_2(bpy)_2(MeCN)_2](PF_6)_2 \cdot 2MeCN$ (6a). Method A. A deep red slurry of **5** (50 mg, 0.066 mmol) was treated with 2 equiv of $NaPF_6$ (22.3 mg, 0.133 mmol) in MeCN (10 mL) and the system heated to reflux for 6 h. Upon cooling, an off-white precipitate. of NaOAc was removed by filtration. The filtrate was layered with Et_2O (25 mL) and slowly produced deep red-orange crystals of **6** in 61% yield.

Method B. In a 25 mL Schlenk flask, **1** (200 mg, 0.377 mmol), bpy (118 mg, 0.755 mmol), and $NaPF_6$ (127 mg, 0.755 mmol) were combined in MeCN (15 mL). The resulting mixture was heated to reflux for 24 h, during which time it slowly converted from deep violet to orange-red. The reaction mixture was cooled and filtered to remove the precipitated NaOAc, and the filtrate was layered with Et_2O (50 mL). This produced deep red-orange crystals of **6** in 74% yield. Anal. Calcd for $C_{28}H_{28}F_{12}N_6O_4P_2Rh_2$: C, 33.35; H, 2.80; N, 8.33. Found: C, 32.92; H, 2.90; N, 8.00. ^{1}H NMR in CD_3CN (ppm): O_2CCH_3, 2.52 (s, 6); bpy, 7.282 (t, 4), 7.710 (d, 4), 7.821 (t, 4), 8.159 (d, 4). IR data (KBr pellet, cm^{-1}): 3121 (w), 3093 (w), 1609 (w), 1559 (s), 1452 (s), 1427 (s), 842 (s, br), 764 (s), 726 (w), 705 (m), 558 (m). Electronic spectrum in MeCN: 218 (33 100), 254 (39 400), 280 (34 400), 298 (27 500), 354 (4740), 408 (2920), 512 (380).

$[Rh_2(O_2CMe)_2(bpy)_2(MeCN)_2](BF_4)_2$ (6b). Complex **1** (200 mg, 0.377 mmol), bpy (118 mg, 0.755 mmol) and $NaBF_4$ (82.9 mg, 0.755 mmol), were combined in MeCN (15 mL), and the resulting deep violet mixture was heated to reflux for 24 h. Upon cooling to room temperature, an off-white precipitate of NaOAc formed. The precipitate was removed by filtration and the resulting filtrate layered with Et_2O (50 mL). The layering slowly produced deep orange crystals of **6b**. The yield was 78%.

$[Rh_2(O_2CEt)_2(bpy)_2(MeCN)_2](PF_6)_2$ (7). Complex **2** (50 mg, 0.089 mmol), bpy (27.8 mg, 0.178 mmol), and $NaPF_6$ (29.9 mg, 0.178 mmol) were combined in MeCN (5 mL), and the mixture was heated to reflux. After 24 h, the mixture was cooled to room temperature and the precipitate of NaO_2CEt removed by filtration. The filtrate was layered with Et_2O (20 mL) to slowly give deep red crystals of **7** in 68% yield. ^{1}H NMR in CD_3CN: $O_2CH_2CH_3$, 1.320 (t, 6); $O_2CH_2CH_3$, 2.727 (q, 4); bpy, 7.301 (t, 4); 7.730 (d, 4), 7.838 (t, 4), 8.130 (d, 4).

(4) (a) Hughes, R. G.; Bear, J. L.; Kimball, A. P. *Proc. Am. Assoc. Cancer Res.* **1972**, *13*, 120. (b) Erck, A.; Rainen, L.; Whileyman, J.; Chang, I.-M.; Kimball, A. P.; Bear, J. *Proc. Soc. Exp. Biol. Med.* **1974**, *145*, 1278. (c) Bear, J. L.; Gray, H. B.; Rainen, L.; Chang, I. M.; Howard, R.; Serio, G.; Kimball, A. P. *Cancer Chemother. Rep.* **1975**, *59*, 611. (d) Howard, R. A.; Spring, T. G.; Bear, J. L. *Cancer Res.* **1976**, *36*, 4402. (e) Erck, A.; Sherwood, E.; Bear, J. L.; Kimball, A. P. *Cancer Res.* **1976**, *36*, 2204. (f) Howard, R. A.; Sherwood, E.; Erck, A.; Kimball, A. P.; Bear, J. L. *J. Med. Chem.* **1977**, *20*, 943. (g) Bear, J. L.; Howard, R. A.; Dennis, A. M. *Curr. Chemother., Proc. Int. Congr. Chemother., 10th, 1977*, **1978**, 1321. (h) Kadish, K. M.; Das, K.; Howard, R.; Dennis, A.; Bear, J. L. *Bioelectrochem. Bioenerg.* **1978**, *5*, 741. (i) Howard, R. A.; Kimball, A. P.; Bear, J. L. *Cancer Res.* **1979**, *39*, 2568. (j) Rao, P. N.; Smith, M. L.; Pathak, S.; Howard, R. A.; Bear, J. L. *J. Natl. Cancer Inst.* **1980**, *64*, 905.

(5) Constable, E. C. *Coord. Chem. Rev.* **1986**, *73*, 59 and references therein.

(6) (a) Perlepes, S. P.; Huffman, J. C.; Matonic, J. H.; Dunbar, K. R.; Christou, G. *J. Am. Chem. Soc.* **1991**, *113*, 2770. (b) Crawford, C. A.; Matonic, J. H.; Streib, W. E.; Huffman, J. C.; Dunbar, K. R.; Christou, G. *Inorg. Chem.* **1993**, *32*, 3125.

(7) (a) Dunbar, K. R.; Matonic, J. H.; Saharan, V. P.; Crawford, C. A.; Christou, G. *J. Am. Chem. Soc.* **1994**, *116*, 2201. (b) Crawford, C. A.; Day, E. F.; Saharan, V. P.; Folting, K.; Huffman, J. C.; Dunbar, K. R.; Christou, G. Submitted for publication.

(8) Halpern, J.; Kimura, E.; Molin-Case, J.; Wong, C. S. *J. Chem. Soc., Chem. Commun.* **1971**, 1207.

(9) (a) Cenini, S.; Ugo, R.; Bonati, F. *Inorg. Chim. Acta* **1967**, *1*, 443. (b) McCarthy, H. J.; Tocher, D. A. *Inorg. Chim. Acta* **1988**, *145*, 171.

(10) McCarthy, H. J.; Tocher, D. A. *Polyhedron* **1989**, *8*, 1117.

(11) (a) Sokol, V. I.; Porai-Koshits, M. A.; Kochetkova, A. P.; Sveshnikova, L. B. *Koord. Khim.* **1984**, *10*, 844. (b) Sokol, V. I.; Porai-Koshits, M. A.; Kochetkova, A. P.; Sveshnikova, L. B. *Sov. J. Coord. Chem.* ***1984****, 10, 461*.

(12) Glowiak, T.; Pasternak, H.; Pruchnik, F. *Acta Crystallogr.* **1987**, *C43*, 1036.

(13) Calligaris, M.; Campana, L.; Mestroni, G.; Tornatore, M.; Alessio, E. *Inorg. Chim. Acta* **1987**, *127*, 103.

(14) Rempel, G. A.; Legzdins, P.; Smith, H.; Wilkinson, G. *Inorg. Synth.* **1972**, *13*, 90.

(15) (a) Cotton, F. A.; Felthouse, T. R. *Inorg. Chem.* **1980**, *19*, 323. (b) Cotton, F. A.; Felthouse, T. R. *Inorg. Chem.* **1981**, *20*, 600.

(16) Crawford, C. A.; Folting, K.; Christou, G. Manuscript in preparation.

$[Rh_2(O_2CPh)_2(bpy)_2(MeCN)_2](PF_6)_2$ (8). Complex **3** (100 mg, 0.145 mmol), bpy (45.3 mg, 0.290 mmol), and $NaPF_6$ (48.7 mg, 0.290 mmol) were combined in MeCN (20 mL), and the deep violet mixture was heated to reflux. After 24 h, the deep red-orange mixture was cooled to room temperature and the precipitate of NaO_2CPh removed by filtration. The filtrate was concentrated to 8 mL and layered with Et_2O (50 mL) to slowly produce deep orange crystals of **8** in 68% yield. ^{1}H NMR in CD_3CN (ppm): O_2CPh, 7.568 (t, 4), 7.680 (t, 2), 8.282 (d, 4); bpy, 7.2463 (t, 4), 7.772 (d, 4), 7.852 (t, 4), 8.211 (d, 4). Electronic spectrum in MeCN: 226 (11 675), 252 (12 576), 304 (12 541), 352 (4082), 402 (2389), 514 (368).

$[Rh_2(O_2CCF_3)_4(bpy)_2]\cdot Me_2CO$ (9). Complex **4** (100 mg, 0.13 mmol) and bpy (40 mg, 0.26 mmol) were dissolved in MeCN (10 mL), and the solution was refluxed for 5 h, after which time the MeCN was removed *in vacuo* and the residue taken up in Me_2CO (10 mL) and layered with hexanes. An orange crystalline solid was slowly obtained, which was collected by filtration and dried *in vacuo*. The yield was 86%. ^{1}H NMR in CD_3CN (ppm): bpy, 7.23 (t), 7.72 (t), 7.81 (d), 8.12 (d). IR data (KBr pellet; cm^{-1}): 1690 (s), 1650 (s), 1610 (m), 1475 (m), 1460 (m), 1435 (m), 1200 (vs), 875 (m), 845 (m), 810 (m), 775 (s), 750 (m), 730 (m). Electronic spectrum in MeCN: 258 (86 000), 305 (68 000), 529 (380).

$[Rh_2(O_2CMe)_2(phen)_2(MeCN)_2](BF_4)_2$ (10). Complex **1** (100 mg, 0.189 mmol), phen (68.1 mg, 0.378 mmol), and $NaBF_4$ were combined in MeCN (8 mL), and the mixture was heated to reflux for 24 h. The mixture was cooled to room temperature and the precipitate of NaOAc removed by filtration. The filtrate was layered with Et_2O (20 mL) to produce red-orange crystals of **10** in 88% yield. ^{1}H NMR in CD_3CN (ppm): O_2CCH_3, 2.57 (s, 6); phen, 8.39 (d, 4), 8.18 (d, 4), 7.63 (s, 4), 7.54 (dd, 4). IR data (KBr pellet, cm^{-1}): 3094 (w), 2936 (w), 1630 (w), 1557 (s), 1518 (m), 1445 (s), 1431 (s), 1414 (s), 1343 (w), 1065 (s, br), 847 (m), 716 (m). Electronic spectrum in MeCN: 224 (14 610), 260 (15 740), 296 (14 530), 362 (4760), 408 (3050), 514 (292).

$[Rh_2(O_2CMe)_2(Me_2bpy)_2(MeCN)_2](BF_4)_2$ (11). This compound was prepared in a manner analogous to that for **10** employing complex **1** (50 mg, 0.099 mmol), Me_2bpy (36.4 mg, 0.198 mmol), and $NaBF_4$ (21.7 mg, 0.198 mmol) in MeCN (5 mL). The yield of **11** was 47%. ^{1}H NMR in CD_3CN (ppm): O_2CCH_3, 2.414 (s, 6); Me_2bpy, 2.452 (s, 12); Me_2bpy, 7.138 (d, 4), 7.637 (s, 4), 7.943 (d, 4). Electronic spectrum in MeCN: 226 (13 714), 254 (14 582), 298 (13 931), 354 (3839), 408 (1995), 526 (246).

$[Rh_2(O_2CMe)_2(Ph_2bpy)_2(MeCN)_2](BF_4)_2$ (12). This compound was prepared in a manner analogous to that for **10**, employing complex **1** (50 mg, 0.099 mmol), Ph_2bpy (61.1 mg, 0.198 mmol), and $NaBF_4$ (21.7 mg, 0.198 mmol) in MeCN (5 mL). The yield of **12** was 85%. ^{1}H NMR in CD_3CN (ppm): O_2CCH_3, 2.524 (s, 6); Ph_2bpy, 7.389 (t, 8), 7.475 (t, 4), 7.610 (m, 12), 8.173 (s, 4), 8.289 (d, 4). Electronic spectrum in MeCN: 224 (17 824), 260 (19 253), 314 (19 115), 370 (7442), 426 (2690), 526 (370).

$[Rh_2(O_2CMe)_2(Ph_2phen)_2(MeCN)_2](BF_4)_2$ (13). Complex **13** was prepared in a manner analogous to that for complex **10**, employing complex **1** (50 mg, 0.099 mmol), Ph_2phen (65.8 mg, 0.198 mmol), and $NaBF_4$ (21.7 mg, 0.198 mmol) in MeCN (8 mL). The yield of **13** was 71%. ^{1}H NMR in CD_3CN (ppm): O_2CCH_3, 2.623 (s, 6); Ph_2phen, 7.241 (d, 8), 7.446 (t, 8), 7.550 (d, 4), 7.601 (d, 4), 7.736 (s, 4), 8.553 (d, 4). Electronic spectrum in MeCN: 224 (11 190), 256 (11 997), 316 (11 424), 358 (10 275), 424 (4040), 526 (386).

$[Rh_2(O_2CMe)_2(bpy)_2(MeCN)_2](BF_4)$ (14). A 0.50 M solution of Na acenaphthylenide was prepared by slowly dissolving Na metal (0.23 g, 0.010 mol) in a solution of acenaphthylene (1.52 g, 0.0100 mol) in THF (20 mL) to give a deep brown solution after stirring overnight. An aliquot of this solution (400 μL, 0.200 mmol) was added via syringe to an orange-red solution of complex **6b** (0.160 g, 0.180 mmol) in MeCN (8 mL); a rapid color change to intense dark blue occurred. Addition of Et_2O (25 mL) precipitated a dark blue solid, which was collected by filtration and washed with Et_2O. The yield was 0.104 g, 72%. A sample dried *in vacuo* analyzed as $[Rh_2(O_2CMe)_2(bpy)_2(MeCN)_{0.5}](BF_4)$. Anal. Calcd for $C_{25}H_{23.5}N_{4.5}BO_4F_4Rh_2$: C, 38.69; H, 3.05; N, 8.12. Found: C, 38.67; H, 3.27; N, 8.20. IR data (KBr pellet, cm^{-1}): 1605 (w), 1553 (m), 1420 (s), 1264 (w), 1055 (s), 802 (w), 760 (m), 723 (m), 698 (m), 669 (m), 517 (w). Electronic spectrum in MeCN: 240 (18 500), 282 (21 500), 582 (15 000), 762 (3600).

$[Rh_2(O_2CPh)(tpy)_2(MeCN)_2](BF_4)_3\cdot MeCN$ (16). In a 25 mL Schlenk flask, complex **15** (0.050 g, 0.042 mmol) was combined with $^nBu_4N(O_2CPh)$ (0.015 g, 0.042 mmol) in MeCN (8 mL) and the resulting mixture stirred for 24 h at room temperature. The solution was filtered and the filtrate layered with Et_2O (25 mL) to slowly produce orange crystals of **16** in 78% yield. X-ray quality crystals were obtained by vapor diffusion of EtO_2CMe into an acetonitrile solution of **16**. ^{1}H NMR in CD_3CN (ppm): $O_2CC_6H_5$, 7.739 (d, 2), 7.848 (t, 1), 8.548 (d, 2); tpy, 7.468 (t, 4), 7.594 (d, 4), 7.951 (d, 4), 8.055 (t, 4), 8.140 (d, 4), 8.165 (t, 2). IR data (KBr pellet, cm^{-1}): 3079 (w), 2320 (w), 2292 (w), 2251 (w), 1605 (m), 1476 (w), 1451 (m), 1402 (w), 1059 (s, br), 775 (s), 521 (m). Electronic spectrum in MeCN: 228 (21 700), 262 (24 200), 310 (19 350), 336 (11 700), 414 (1690), 492 (250).

X-ray Crystallography and Structure Solution. Data were collected on $[Rh_2(OAc)_2(bpy)_2(MeCN)_2](PF_6)_2\cdot 2MeCN$ (**6a**) and $[Rh_2(O_2CPh)(tpy)_2(MeCN)_2](BF_4)_3\cdot MeCN$ (**16**) using a Picker four-circle diffractometer; details of the diffractometry, low-temperature facilities, and computational procedures employed by the Molecular Structure Center are available elsewhere.[17] For $[Rh_2(O_2CCF_3)_4(bpy)_2]\cdot Me_2CO$ (**9**), data were collected on a Rigaku AFC6S diffractometer. General procedures are described elsewhere,[18] and the structure solution and refinement were carried out using the software package TEXSAN.[19] Three or four standard reflections measured periodically throughout data collection revealed negligible decay for **6a** and **16** but a 65% decay for **9**, attributed to loss of interstitial Me_2CO molecules; a linear decay correction was applied to compensate for this decay. In addition, an empirical absorption correction for **9** was applied on the basis of three ψ-scans which gave transmission factors ranging from 0.88 to 1.00.

For complex **6a**, a systematic search of a limited hemisphere of reciprocal space located a set of diffraction maxima with Laue symmetry corresponding to the unique monoclinic space group $P2_1/a$ (alternate setting of $P2_1/c$). Subsequent solution and refinement of the structure confirmed this choice. The structure was solved by a combination of direct methods (MULTAN78) and Fourier techniques. After all non-hydrogen atoms had been located, a Fourier difference map revealed the location of some, but not all, of the hydrogen atoms. All hydrogen atom positions were therefore calculated using idealized geometries and $d(C-H) = 0.95$ Å. These calculated positions were fixed for the final cycles of refinement, which involved anisotropic and isotropic thermal parameters for non-hydrogen and hydrogen atoms, respectively. A final Fourier difference map was featureless, with the largest peak being 0.74 e/Å^3.

For complex **9**, the structure was solved using the TEXSAN software package. The positions of the rhodium atoms were taken from a direct methods *E*-map whereas all other atoms were located from a series of Fourier difference maps and full-matrix least-squares refinement cycles. The atoms in the trifluoroacetate groups, particularly those in the axial positions, were characterized by the usual high thermal motion; thus it was necessary to refine them with isotropic thermal parameters. In fact, because of the limited amount of observed data owing to the weak diffraction properties of the crystal, only the Rh atoms, and most of the atoms directly bound to them, were refined anisotropically.

For complex **16**, a systematic search of a limited hemisphere of reciprocal space yielded a set of reflections which exhibited no symmetry (other than $\bar{1}$) and no systematic extinctions. The initial choice of the centrosymmetric space group $P\bar{1}$ was confirmed by the subsequent solution and refinement of the structure. The structure was solved using a combination of direct methods (SHELXS-86) and Fourier techniques. The Rh atoms and some other parts of the cation were obtained initially; the remaining atoms, including almost all of the hydrogen atoms, were obtained from iterations of least-squares refinement and difference Fourier map calculations. The asymmetric unit was found to contain the Rh_2 cation, three BF_4 anions, and some disordered CH_3CN solvent molecules situated near a center of symmetry. In the final cycles of refinement, the non-hydrogen atoms in

(17) Chisholm, M. H.; Folting, K.; Huffman, J. C.; Kirkpatrick, C. C. *Inorg. Chem.* **1984**, *23*, 1021.
(18) (a) Cotton, F. A.; Frenz, B. A.; Deganello, G.; Shaver, A. *J. Organomet. Chem.* **1973**, 227. (b) Bino, A.; Cotton, F. A.; Fanwick, P. E. *Inorg. Chem.* **1979**, *18*, 3558.
(19) TEXSAN-TEXRAY Structure Analysis package, Molecular Structure Corp., 1985.

Table 1. Crystallographic Data for $[Rh_2(Oac)_2(MeCN)_2](PF_6)_2$, 2MeCN (**6a**), $[Rh_2(O_2CCF_3)_4(bpy)_2]\cdot Me_2CO$ (**9**), and $[Rh_2(O_2CPh)(tpy)_2(MeCN)_2](BF_4)_3\cdot MeCN$ (**16**)

	6a	**9**	**16**
formula[a]	$C_{32}H_{34}N_8O_4F_{12}P_2Rh_2$	$C_{31}H_{22}N_4O_9F_{12}Rh_2$	$C_{41}H_{33}B_3F_{12}N_8O_2Rh_2$
fw, g/mol	1090.41	1030.34	1135.99
space group	$P2_1/a$	$P\bar{1}$	$P\bar{1}$
a, Å	14.433(2)	14.260(4)	11.684(4)
b, Å	12.810(1)	15.375(4)	20.373(8)
c, Å	22.178(3)	9.709(2)	10.451(3)
α, deg	90	105.98(2)	93.47(2)
β, deg	104.42(3)	97.49(2)	110.53(1)
γ, deg	90	70.32(2)	100.03(2)
V, Å^3	3971.2	1925.2	2274.1
Z	4	2	2
T, °C	−172	20	−168
radiation[b]	Mo Kα	MoKα	MoKα
ρ_{calc}, g/cm^3	1.824	1.777	1.659
μ, cm^{-1}	9.990	9.526	8.058
octants	$+h, +k, \pm l$	$+h, \pm k, \pm l$	$+h, \pm k, \pm l$
unique data	5206	5103	5983
obsd data	3569[c]	1657[d]	4844[d]
R (R_w)[e]	0.0695 (0.0750)	0.097 (0.118)	0.0446 (0.0452)

[a] Including solvate molecules. [b] Graphite monochromator. [c] $F > 2.33\sigma(F)$. [d] $I > 3\sigma(I)$. [e] $R = \sum||F_o| - |F_c||/\sum|F_o|$. $R_w = [\sum w(|F_o| - |F_c|)^2/\sum w|F_o|^2]^{1/2}$ where $w = 1/\sigma^2(|F_o|)$.

the cation and anions were varied with anisotropic thermal parameters and the solvent atoms were refined using isotropic thermal parameters and an occupancy factor. The hydrogen atoms were kept in fixed idealized positions. The final difference map was reasonably clean; the largest peak was 1.2 e/Å^3 in the area of the disordered solvent, and the deepest hole was −0.6 e/Å^3. No correction was made for absorption. Final R (R_w) values are listed in Table 1.

Other Measurements. Infrared (KBr pellets) and solution electronic spectra were recorded on Nicolet Model 510P and Hewlett-Packard Model 8452A spectrophotometers, respectively. Electrochemistry was performed with a BAS Model CV-50W instrument employing a standard three-electrode cell (glassy carbon working, Pt wire auxiliary, and SCE reference electrodes). The supporting electrolyte was $NBu^n_4PF_6$. Potentials are quoted *vs* the ferrocene/ferrocenium couple as an internal standard (0.33 V *vs* SCE under our conditions). Controlled potential electrolysis was performed with a Pt basket and Pt mesh working and auxiliary electrodes. ^{1}H NMR spectra were recorded on Varian XL-300 and Bruker AM-500 MHz spectrometers. EHT calculations were performed on $[Rh_2(O_2CH)_2(bpy)_2(HCN)_2]^{2+}$ and $[Rh_2(O_2CH)(tpy)_2(HCN)_2]^{3+}$ using weighted H_{ij}'s; atomic coordinates were taken from the structures of **6a** and **16**.

Results and Discussion

Syntheses. In previous work, it had been shown that reaction of $[Rh_2(O_2CMe)_4(MeOH)_2]$ (**1**) in Me_2CO with 1 equiv of bpy leads to precipitation in almost quantitative yield of green $Rh_2(O_2CMe)_4(bpy)$, which contains an axial−equatorial (*ax*−*eq*) bpy group.[6b] In MeCN, the product precipitates more slowly and in a more modest yield (∼40%).[6a] In the latter solvent, addition of a second 1 equiv of bpy does not appear to affect the reaction, a green precipitate of the same mono-bpy product being obtained. However, very careful examination of green powders from the MeCN reactions reveals trace amounts of orange specks which were suspected of being a bis(bpy) product. A search for higher yields of such a product was therefore initiated and readily developed. It was soon realized that reaction with a second 1 equiv of bpy does occur, but it is slow at room temperature and is thus facilitated by elevated temperatures. Thus, complex **1** was treated with 2 equiv of bpy in refluxing MeCN for 24 h; a color change occurred with loss of the intense violet color of **1** and formation of a brick-red precipitate with a formulation from elemental analysis of $Rh_2(O_2CMe)_4(bpy)_2$; on the basis of the low solubility and the subsequent identification of **6** (*vide infra*), this compound is better formulated as $[Rh_2(O_2CMe)_2(bpy)_2](O_2CMe)_2$ (**5**). In order to obtain suitable crystals for firm, crystallographic determination of the structure, more soluble forms were sought and attained by addition of $NaPF_6$ or $NaBF_4$ to the reaction mixtures; this gave a precipitate of NaO_2CMe and an orange-red solution, from which was subsequently isolated the $[Rh_2(O_2CMe)_2(bpy)_2(MeCN)_2]^{2+}$ ion as the PF_6^- (**6a**) and BF_4^- (**6b**) salts. In a complementary approach, **5** was dissolved slowly in refluxing MeCN containing $NaPF_6$ to give NaO_2CMe and an orange-red solution, from which was isolated **6a** (method A). These reactions are summarized in eqs 1 and 2. The one-

$$\underset{\mathbf{1}}{Rh_2(O_2CMe)_4(MeOH)_2} + 2bpy \xrightarrow[-MeOH]{MeCN} \underset{\mathbf{5}}{[Rh_2(O_2CMe)_2(bpy)_2](O_2CMe)_2} \quad (1)$$

$$\underset{\mathbf{5}}{[Rh_2(O_2CMe)_2(bpy)_2](O_2CMe)_2} + 2NaPF_6 \xrightarrow{MeCN} \underset{\mathbf{6a}}{[Rh_2(O_2CMe)_2(bpy)_2](PF_6)_2} + 2NaO_2CMe \quad (2)$$

pot reaction involving addition of $NaPF_6$ (method B) or $NaBF_4$ is the more convenient one and has been employed in all subsequent reactions: the same procedure with phen, Me_2bpy, Ph_2bpy, and Ph_2phen readily gives complexes **10**, **11**, **12**, and **13**, respectively; similarly, reactions of bpy with complexes **2** (R = Et), **3** (R = Ph), and **4** (R = CF_3) gives complexes **7**, **8**, and **9**, respectively. Thus, this procedure has allowed a family of $[Rh_2(O_2CR)_2(N\text{-}N)_2]^{2+}$ complexes to be attained with a variety of carboxylates and chelates. The preparation of complex **14**, the one-electron-reduced version of **6b**, will be described in a later section (*vide infra*). Crystallographic studies were performed on complexes **6a** and **9**, the latter because it is of interest to assess the structural consequences of the presence of the strongly-electron-withdrawing CF_3 group.

Once certain properties of the $[Rh_2(O_2CR)_2(N\text{-}N)_2]^{2+}$ complexes had become known (*vide infra*), it became of interest to extend this work to complexes containing tridentate rather than bidentate N-based chelates, and the chelate chosen was 2,2′:6′,2″-terpyridine (tpy). The complex $[Rh_2(O_2CPh)(tpy)_2(MeCN)_2](BF_4)_3\cdot MeCN$ (**16**) was obtained by the reaction in MeCN of equimolar amounts of $NBu^n_4(O_2CPh)$ and $[Rh_2(tpy)_2(MeCN)_4](BF_4)_4$ (**15**), as summarized in eq 3. Complex **15** was itself

$$\underset{\mathbf{15}}{[Rh_2(tpy)_2(MeCN)_4](BF_4)_4} + NBu^n_4(O_2CPh) \xrightarrow{MeCN} \underset{\mathbf{16}}{[Rh_2(O_2CPh)(tpy)_2(MeCN)_2](BF_4)_3\cdot MeCN} \quad (3)$$

prepared by reaction of $[Rh_2(MeCN)_{10}](BF_4)_4$[20] with 2 equiv of tpy. The reaction of eq 3 provides a clean and high-yield route to **16**, which was structurally characterized as **16**·MeCN; attempts to prepare **16** in a manner analogous to that used to prepare **5** and **6** have not as yet resulted in clean yields of product.

Description of Structures. The structures of the cation of **6a**, complex **9**, and the cation of complex **16** are shown in Figures 1, 2, and 3, respectively; fractional coordinates and selected metric parameters are listed in Tables 2−7.

Complex **6a** crystallizes in monoclinic space group $P2_1/a$, with the asymmetric unit containing the entire cation, two PF_6^- anions, and two lattice MeCN molecules; the latter four units

(20) (a) Dunbar, K. R. *J. Am. Chem. Soc.* **1988**, *110*, 8247. (b) Dunbar, K. R.; Pence, L. E. *Inorg. Synth.* **1992**, *29*, 182.

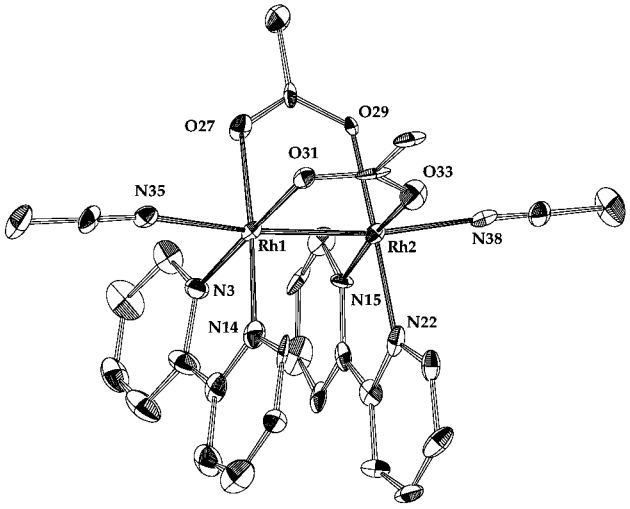

Figure 1. ORTEP representation of the cation of complex **6a** at the 50% probability level. Carbon atoms are numbered sequentially around from N and O atoms.

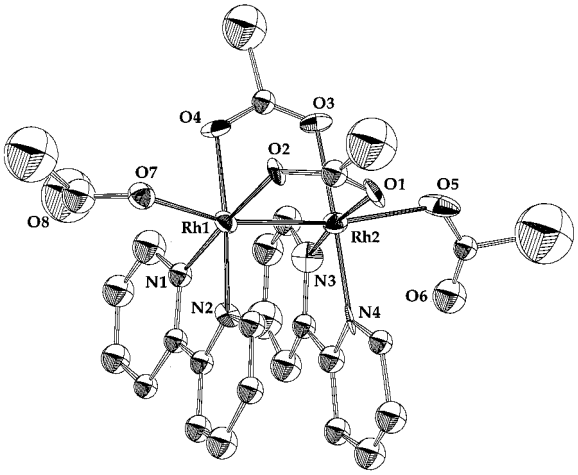

Figure 2. ORTEP representation of complex **9**; F atoms are omitted for clarity.

are unremarkable and will not be discussed. The cation consists of two chelating, *eq*−*eq* bpy groups attached to two Rh atoms in a *syn* disposition; the remaining equatorial sites are occupied by two bridging $MeCO_2^-$ groups. Two MeCN groups at the axial positions and a Rh−Rh single bond (2.548(4) Å) complete six-coordination at each metal atom. The cation has idealized C_{2v} symmetry. The presence of two bridging $MeCO_2^-$ ligands results in retention of an eclipsed conformation about the Rh−Rh single bond; for example, the N(3)−Rh(1)−Rh(2)−N(15) torsional angle is only 6.2°. As expected, the axial Rh−N bonds (2.185(9), 2.228(9) Å) are significantly longer than equatorial Rh−N bonds (1.984(10)−2.003(10) Å).

The eclipsed conformation, the *syn* disposition of the bpy ligands, and the Rh−Rh separation of 2.548(4) Å would result in the bpy planes being much closer than acceptable for π-stacking contacts (*ca*. 3.3−3.5 Å) if the equatorial planes of the two Rh atoms remained parallel. Unfavorably short bpy⋯bpy contacts are prevented, however, by a movement apart or splaying of the bpy groups, resulting in a dihedral angle of 15.8° between the N(3), N(14), O(27), O(31) and N(15), N(26), O(29), O(33) least-squares planes, with the bpy planes remaining essentially coplanar with these equatorial planes. As a consequence of this splaying, the average bpy⋯bpy distance is 3.47 Å, a favorable π-stacking distance between two such π-systems. Similar splaying has been reported in the structures of $[Rh_2(O_2CR)_2(phen)_2Cl_2]$ (and substituted-phen derivatives) possessing two *syn*-phen groups.[13]

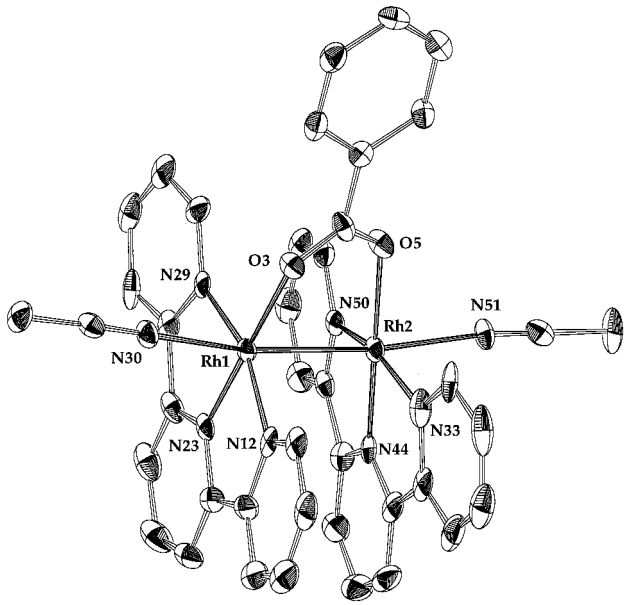

Figure 3. ORTEP representation of the cation of complex **16** at the 50% probability level. Carbon atoms are numbered sequentially around from N and O atoms, and hydrogen atoms have been omitted for clarity.

The structure of complex **9** is very similar to that of **6a**. The conformation is again essentially eclipsed (N(1)−Rh(1)−Rh(2)-N(3) = 11.6°), the bpy groups are *syn*, and two $CF_3CO_2^-$ groups are bridging. The bpy groups are again splayed (dihedral angle between the two equatorial planes = 11.7°). The major difference between **9** and **6a** is the identity of the axial ligands, which in **9** are two additional $CF_3CO_2^-$ groups; this gives a molecular or, better, a tightly ion-paired description of **9**, the axial Rh−O_2CCF_3 linkages not being expected to be maintained in solution in a fairly good donor solvent.

Complex **16** crystallizes in monoclinic space group $P\bar{1}$ with no crystallographically-imposed symmetry, but with a cation of idealized C_2 symmetry. The two Rh centers are bridged by a benzoate ligand in the familiar $\eta^1{:}\eta^1{:}\mu$ binding mode which spans the Rh−Rh bond of 2.629(1) Å. The coordination at each metal center is completed by a tridentate tpy ligand bound in the equatorial plane, an axial MeCN molecule, and the second metal center. The tpy ligands are bound asymmetrically to the Rh atoms with the Rh−N bonds to the central pyridyl nitrogen atoms (Rh(1)−N(23) and Rh(2)−N(44)) approximately 0.1 Å shorter than those Rh−N bonds to the outer rings (Rh(1)−N(12), Rh(1)−N(29), Rh(2)−N(33), and Rh(1)−N(50)). This probably results from the small bite angle between the end py groups of the tpy ligand (N(12)−Rh(1)−N(29) = 160.70(21)° and N(33)−Rh(2)−N(50) = 161.06(21)°). Additionally, the planes defined by the two tpy ligands form a dihedral angle of only 4.2°, assignable to the relative inflexibility of this tridentate ligand which prevents the splaying seen with the bidentate chelates. The resultant unfavorably short tpy⋯tpy separations are relieved slightly by a stretching of the Rh−Rh bond to an unusually long value (2.629(1) Å). The presence of a single bridging carboxylate ligand is insufficient to retain the approximately eclipsed geometry about the Rh−Rh bond observed in $[Rh_2(O_2CR)_4L_2]$ and $[Rh_2(O_2CR)_2(N\text{-}N)_2]^{2+}$ complexes, and **16** consequently has a more staggered conformation with an average torsion angle of 21.6°. Recently, the related complex $[Rh_2(O_2CMe)(tpy)_2Cl_2]$ has been reported, and it is very similar to **16**

Table 2. Selected Fractional Coordinates ($\times 10^4$) and Equivalent Isotropic Thermal Parameters (Å^2, $\times 10$)[a] for $[Rh_2(O_2CMe)_2(bpy)_2(MeCN)_2](PF_6)_2 \cdot 2MeCN$ (**6a**)

atom	*x*	*y*	*z*	B_{eq}
Rh(1)	3532(1)	4977(1)	3086.7(4)	10
Rh(2)	5213(1)	4956(1)	3804.4(4)	10
N(3)	3730(7)	3898(8)	2477(5)	17
C(4)	3628(8)	2873(9)	2532(6)	17
C(5)	3649(9)	2190(10)	2063(6)	21
C(6)	3813(9)	2568(11)	1520(7)	29
C(7)	3938(9)	3624(12)	1455(6)	28
C(8)	3881(9)	4300(9)	1941(6)	18
C(9)	3939(9)	5411(11)	1920(6)	24
C(10)	4096(10)	5995(12)	1428(6)	28
C(11)	4124(10)	7064(11)	1463(6)	25
C(12)	3975(10)	7563(11)	1972(6)	29
C(13)	3834(10)	6954(10)	2468(6)	23
N(14)	3820(7)	5901(7)	2437(5)	15
N(15)	5763(7)	4003(8)	3280(5)	17
C(16)	5786(8)	2962(9)	3324(5)	15
C(17)	6112(9)	2344(9)	2906(6)	23
C(18)	6436(9)	2841(10)	2437(6)	21
C(19)	6423(9)	3878(10)	2403(6)	20
C(20)	6122(8)	4464(9)	2830(6)	14
C(21)	6164(8)	5613(9)	2898(6)	14
C(22)	6556(8)	6263(10)	2521(6)	18
C(23)	6592(9)	7327(9)	2655(7)	25
C(24)	6240(8)	7710(9)	3116(6)	19
C(25)	5839(9)	7052(9)	3470(6)	17
N(26)	5788(7)	6007(7)	3342(4)	11
O(27)	3184(5)	3941(6)	3698(4)	13
C(28)	3834(10)	3543(9)	4126(6)	18
O(29)	4690(6)	3771(6)	4243(4)	21
C(30)	3550(9)	2720(9)	4532(6)	18
O(31)	3272(6)	6134(6)	3651(4)	15
C(32)	3852(8)	6402(9)	4140(5)	11
O(33)	4705(5)	6051(6)	4312(3)	13
C(34)	3588(10)	7242(10)	4528(6)	22
N(35)	2008(6)	5005(8)	2548(4)	14
C(36)	1276(8)	5003(10)	2203(5)	18
C(37)	339(8)	4981(11)	1775(6)	27
N(38)	6547(6)	4948(8)	4534(4)	15
C(39)	7286(8)	4996(10)	4888(5)	18
C(40)	8181(9)	4995(12)	5343(6)	29

[a] $B_{eq} = (4/3)\sum\sum B_{ij} a_i a_j$.

with a Rh−Rh bond length of 2.634(1) Å and a torsion angle involving the tpy rings of 23° away from an eclipsed conformation.[21]

^{1}H NMR Spectroscopy. The ^{1}H NMR spectrum of complex **6b** in CD_3CN is as expected for retention of the solid-state structure of **6a** on dissolution in this solvent. Analogous spectra were obtained and similar conclusions were reached for complexes **7**−**13**. The representative spectrum of complex **6b** is shown in Figure 4; the effective C_{2v} symmetry leads to four bpy resonances in the aromatic region and a single $MeCO_2^-$ resonance at 2.45 ppm. The axial MeCN ligands exchange rapidly with bulk solvent on the ^{1}H NMR time scale, and a single resonance for free MeCN (1.93 ppm) is observed immediately on dissolution. The complex is stable in solution, its spectrum not changing with time; the complex is also stable in other polar solvents (H_2O, MeOH, DMSO, and pyridine) as judged by ^{1}H NMR spectroscopy. The combined NMR data are collected for convenience in Table 8.

Electrochemistry. The electrochemical properties of complexes **6**−**13** have been investigated by cyclic voltammetry (CV) and differential pulse voltammetry (DPV) in MeCN. The results for complex **6b** are shown in Figure 5. There are a reversible one-electron reduction at −0.89 V and two irreversible processes, one being a second reduction at ∼−1.8 V and the other an oxidation at ∼+1.4 V. The CV scan has $i_f/i_r \approx 1$ (f = forward, r = reverse), and a plot of i_f *vs* $\nu^{1/2}$ gave a straight line for the scan rate (ν) range 50−500 mV/s, indicating a diffusion-controlled process. The peak separation (Δp) is rather large (∼190 mV) when compared with that for ferrocene under the same experimental conditions (∼130 mV), and the return wave is less steep than the forward wave; the latter asymmetry is likely due to a small structural change that accompanies reduction (*vide infra*). The nature and reversibility of the reduction process were further probed by controlled potential electrolysis (CPE) at −0.99 V: coulometry showed the reduction to be a one-electron process ($n \approx 1.0$), and the electrolysis caused a color change from the orange-red of $[Rh_2(O_2CMe)_2(bpy)_2]^{2+}$ to a stable dark blue, indicating the reduction product to be stable on a longer time scale. Further, the CV and DPV of the reduced product, generated by CPE or preisolated (*vide infra*), now gave an oxidation process at the same potential within experimental error. These observations suggest that the reduced material remains dinuclear with essentially the same structure as the parent $[Rh_2(O_2CMe)_2(bpy)_2]^{2+}$ cation. Similar

Table 3. Selected Fractional Coordinates ($\times 10^4$) and Equivalent[a] or Actual Isotropic Thermal Parameters (Å^2, $\times 10$) for $[Rh_2(O_2CCF_3)_4(bpy)_2] \cdot Me_2CO$ (**9**)

atom	*x*	*y*	*z*	B_{iso}/B_{eq}
Rh(1)	0.2247(3)	0.4304(2)	0.1458(4)	3.0
Rh(2)	0.2813(3)	0.2842(2)	0.2520(4)	3.2
O(1)	0.134(2)	0.318(2)	0.290(2)	4
O(2)	0.089(2)	0.463(2)	0.239(3)	3
O(3)	0.297(2)	0.379(2)	0.446(2)	4
O(4)	0.276(2)	0.496(2)	0.347(3)	5
O(5)	0.302(2)	0.172(2)	0.378(3)	6
O(6)	0.403(3)	0.052(2)	0.239(3)	6.6(8)
O(7)	0.156(2)	0.572(2)	0.107(3)	4
O(8)	0.299(5)	0.602(4)	0.102(6)	16(2)
N(1)	0.352(2)	0.393(2)	0.049(3)	3.1(7)
N(2)	0.179(3)	0.372(2)	−0.058(3)	3
N(3)	0.424(2)	0.236(2)	0.213(4)	4
N(4)	0.276(2)	0.193(2)	0.066(3)	2
C(1)	0.430(4)	0.421(3)	0.109(5)	6(1)
C(2)	0.520(4)	0.388(3)	0.029(5)	6(1)
C(3)	0.525(3)	0.336(3)	−0.109(4)	5(1)
C(4)	0.434(3)	0.314(3)	−0.175(4)	3.2(9)
C(5)	0.348(3)	0.348(3)	−0.090(4)	3.5(9)
C(6)	0.252(3)	0.337(3)	−0.149(4)	3.0(9)
C(7)	0.233(3)	0.296(3)	−0.293(4)	4(1)
C(8)	0.138(4)	0.293(3)	−0.338(5)	6(1)
C(9)	0.063(3)	0.330(3)	−0.236(4)	4(1)
C(10)	0.087(4)	0.371(3)	−0.092(4)	4(1)
C(11)	0.493(4)	0.262(3)	0.296(5)	4(1)
C(12)	0.591(4)	0.225(3)	0.258(5)	5(1)
C(13)	0.613(4)	0.166(4)	0.120(6)	8(1)
C(14)	0.542(4)	0.131(3)	0.018(5)	5(1)
C(15)	0.446(3)	0.177(3)	0.078(4)	3.0(9)
C(16)	0.365(3)	0.150(3)	0.003(4)	4(1)
C(17)	0.373(3)	0.084(3)	−0.136(4)	4(1)
C(18)	0.282(4)	0.063(3)	−0.189(4)	5(1)
C(19)	0.195(4)	0.100(3)	−0.130(5)	6(1)
C(20)	0.189(3)	0.173(3)	0.012(4)	3.2(9)
C(21)	0.297(3)	0.455(3)	0.447(5)	3(1)
C(23)	0.071(3)	0.402(3)	0.275(4)	4(1)
C(25)	0.210(5)	0.622(4)	0.077(6)	6(1)
C(27)	0.344(4)	0.094(3)	0.328(5)	3(1)
C(31)	0.90(2)	0.11(2)	0.33(3)	23.8(8)
O(10)	0.88(1)	0.09(1)	0.29(1)	17(1)
C(30)	0.97(1)	0.076(8)	0.23(1)	10(2)
C(32)	0.94(1)	0.136(8)	0.45(1)	10(2)
C(24)	−0.039(2)	0.424(2)	0.324(3)	14.9(8)
C(28)	0.335(3)	0.020(2)	0.416(3)	20(1)
C(22)	0.317(2)	0.528(1)	0.590(2)	11.1(5)
C(26)	0.150(2)	0.731(2)	0.102(3)	16.4(8)

[a] $B_{eq} = (4/3)\sum\sum B_{ij} a_i a_j$.

(21) Pruchnik, F. P.; Robert, F.; Jeannin, Y.; Jeannin, S. *Inorg. Chem.* **1996**, *35*, 4261.

Table 4. Selected Fractional Coordinates ($\times 10^4$) and Equivalent Isotropic Thermal Parameters ($Å^2$, $\times 10$)[a] for $[Rh_2(O_2(CPh)(terpy)_2(MeCN)_2](BF_4)_3 \cdot MeCN$ (**16**)

atom	*x*	*y*	*z*	B_{eq}
Rh(1)	3326.7(4)	2997.1(2)	4403.8(5)	13
Rh(2)	1279.0(4)	2722.5(2)	4955.1(5)	14
O(3)	3539(4)	3926(2)	5484(4)	17
C(4)	3044(6)	3972(3)	6377(6)	18
O(5)	2195(4)	3525(2)	6482(4)	19
C(6)	3501(6)	4599(3)	7387(6)	16
C(7)	4549(6)	5064(3)	7479(7)	19
C(8)	4959(6)	5636(3)	8454(7)	23
C(9)	4340(6)	5736(3)	9326(6)	22
C(10)	3308(6)	5267(3)	9261(7)	21
C(11)	2875(6)	4705(3)	8279(7)	19
N(12)	2402(4)	3163(3)	2425(5)	17
C(13)	2174(6)	3741(4)	1975(7)	22
C(14)	1570(6)	3777(4)	581(8)	27
C(15)	1254(6)	3217(4)	−367(7)	31
C(16)	1508(6)	2617(4)	89(7)	26
C(17)	2100(6)	2606(3)	1480(6)	21
C(18)	2462(6)	1994(3)	2070(6)	20
C(19)	2203(6)	1346(4)	1392(7)	25
C(20)	2653(7)	850(3)	2132(8)	29
C(21)	3354(7)	988(3)	3531(8)	27
C(22)	3584(6)	1639(3)	4177(7)	19
N(23)	3116(4)	2117(2)	3449(5)	15
C(24)	4302(6)	1895(3)	5649(7)	18
C(25)	4990(6)	1532(4)	6604(8)	25
C(26)	5651(6)	1835(4)	7939(7)	26
C(27)	5667(6)	2503(4)	8304(7)	25
C(28)	4991(6)	2843(3)	7316(6)	21
N(29)	4303(4)	2552(3)	6022(5)	15
N(30)	5082(5)	3374(3)	4189(5)	18
C(31)	6042(6)	3533(3)	4108(6)	17
C(32)	7248(6)	3724(4)	3960(7)	23
N(33)	344(5)	3229(3)	3427(6)	22
C(34)	308(6)	3883(4)	3492(8)	25
C(35)	−428(7)	4139(4)	2356(9)	33
C(36)	−1094(7)	3730(4)	1133(8)	33
C(37)	−1071(6)	3059(4)	1071(8)	29
C(38)	−370(6)	2802(4)	2212(7)	22
C(39)	−315(5)	2094(3)	2264(7)	20
C(40)	−907(6)	1555(4)	1217(7)	28
C(41)	−738(6)	916(4)	1493(7)	27
C(42)	−37(6)	803(3)	2777(7)	23
C(43)	546(6)	1347(3)	3809(7)	19
N(44)	411(4)	1969(3)	3504(5)	17
C(45)	1316(6)	1340(3)	5266(6)	17
C(46)	1537(6)	756(3)	5845(7)	22
C(47)	2237(6)	805(4)	7250(7)	25
C(48)	2698(6)	1435(4)	8032(7)	21
C(49)	2453(6)	1985(3)	7401(6)	18
N(50)	1801(4)	1957(2)	6041(5)	14
N(51)	−318(5)	2629(3)	5604(5)	18
C(52)	−1182(6)	2523(3)	5854(6)	19
C(53)	−2320(6)	2375(4)	6185(8)	30

[a] $B_{eq} = (4/3)\sum\sum B_{ij} a_i a_j$.

CV and DPV studies on complexes **7**−**13** gave analogous results for **7**, **8**, **10**, and **11** but slightly different ones for **12** and **13**. The results are presented in Table 9. Complex **9** led to only irreversible processes and is not included; its atypical behavior is assigned to the greater lability of the $CF_3CO_2^-$ groups.

Reversible oxidations of $[Rh_2]^{4+}$ complexes are relatively common and well-investigated, with the assignment of the redox process to a formally metal-based oxidation to give a $[Rh_2]^{5+}$ unit being widely accepted and supported by a variety of data.[2h] In contrast, reversible or quasi-reversible reductions of $[Rh_2]^{4+}$ complexes to $[Rh_2]^{3+}$ species (i.e., formally at the Rh^IRh^{II} oxidation level) are relatively rare, in part due to the difficulty of reducing the $[Rh_2]^{4+}$ core. Such procedures have, however, been developed in several instances by employing, for example, electrochemical reduction[22] or γ-irradiation methods.[23] More common as a route to $[Rh_2]^{3+}$ species are oxidations of $[Rh^I_2]^{2+}$ species, especially those containing π-bonding ligands such as CO, isocyanides, or unsaturated hydrocarbons.[24] EPR spectra of such $[Rh_2]^{3+}$ species are consistent with the added electron entering a LUMO that is Rh−Rh σ^* in character, i.e., a formal Rh^IRh^{II} oxidation state description.[22−24] In this regard, it is relevant to remember that Rh−Rh bonding in the $[Rh_2]^{4+}$ unit

Table 5. Selected Bond Distances (Å) and Angles (deg) for $[Rh_2(O_2CMe)_2(bpy)_2(MeCN)_2](PF_6)_2 \cdot 2MeCN$ (**6a**)

(a) Bonds

Rh(1)−Rh(2)	2.548(1)	Rh(2)−O(29)	2.046(9)
Rh(1)−O(27)	2.048(8)	Rh(2)−O(33)	2.044(8)
Rh(1)−O(31)	2.035(8)	Rh(2)−N(15)	1.984(11)
Rh(1)−N(3)	2.003(10)	Rh(2)−N(26)	1.994(10)
Rh(1)−N(14)	1.986(10)	Rh(2)−N(38)	2.185(8)
Rh(1)−N(35)	2.228(8)		

(b) Angles

Rh(2)−Rh(1)−N(3)	98.1(3)	O(27)−Rh(1)−N(35)	89.6(3)
Rh(2)−Rh(1)−N(14)	96.9(3)	O(31)−Rh(1)−N(3)	175.7(3)
Rh(2)−Rh(1)−N(35)	174.1(3)	O(31)−Rh(1)−N(14)	96.7(4)
Rh(2)−Rh(1)−O(27)	86.1(2)	O(31)−Rh(1)−N(35)	90.5(3)
Rh(2)−Rh(1)−O(31)	85.2(2)	N(3)−Rh(1)−N(14)	80.3(4)
Rh(1)−Rh(2)−N(15)	95.6(3)	N(3)−Rh(1)−N(35)	86.4(4)
Rh(1)−Rh(2)−N(26)	97.2(3)	N(14)−Rh(1)−N(35)	87.6(4)
Rh(1)−Rh(2)−N(38)	171.4(3)	O(29)−Rh(2)−O(33)	91.3(3)
Rh(1)−Rh(2)−O(29)	84.2(2)	O(29)−Rh(2)−N(15)	94.0(4)
Rh(1)−Rh(2)−O(33)	85.5(2)	O(29)−Rh(2)−N(26)	174.5(4)
O(27)−Rh(1)−O(31)	87.2(3)	O(29)−Rh(2)−N(38)	90.3(3)
O(27)−Rh(1)−N(3)	95.7(4)	O(33)−Rh(2)−N(15)	174.7(4)
O(27)−Rh(1)−N(14)	175.2(3)	O(33)−Rh(2)−N(26)	94.2(4)
O(33)−Rh(2)−N(38)	88.1(3)	N(15)−Rh(2)−N(38)	91.4(4)
N(15)−Rh(2)−N(26)	80.5(4)	N(26)−Rh(2)−N(38)	88.9(4)

Table 6. Selected Bond Distances (Å) and Angles (deg) for $[Rh_2(O_2CCF_3)_4(bpy)_2] \cdot Me_2CO$ (**9**)

(a) Bonds

Rh(1)−Rh(2)	2.570(6)	Rh(2)−O(1)	2.05(3)
Rh(1)−O(2)	2.10(3)	Rh(2)−O(3)	2.07(2)
Rh(1)−O(4)	2.10(3)	Rh(2)−O(5)	2.30(4)
Rh(1)−O(7)	2.19(3)	Rh(2)−N(3)	1.97(4)
Rh(1)−N(1)	1.99(3)	Rh(2)−N(4)	1.97(3)
Rh(1)−N(2)	2.06(3)		

(b) Angles

Rh(2)−Rh(1)−O(2)	85.2(8)	Rh(1)−Rh(2)−O(1)	85.2(9)
Rh(2)−Rh(1)−O(4)	82.9(8)	Rh(1)−Rh(2)−O(3)	85.8(8)
Rh(2)−Rh(1)−O(7)	165.1(7)	Rh(1)−Rh(2)−O(5)	167.5(7)
Rh(2)−Rh(1)−N(1)	93(1)	Rh(10)−Rh(2)−N(3)	100(1)
Rh(2)−Rh(1)−N(2)	100.8(9)	Rh(1)−Rh(2)−N(4)	94(1)
O(2)−Rh(1)−O(4)	87(1)	O(1)−Rh(2)−O(3)	89(1)
O(2)−Rh(1)−O(7)	83(1)	O(1)−Rh(2)−O(5)	84(1)
O(2)−Rh(1)−N(1)	176(1)	O(1)−Rh(2)−N(3)	174(1)
O(2)−Rh(1)−N(2)	96(1)	O(7)−Rh(1)−N(1)	99(1)
O(4)−Rh(1)−O(7)	88(1)	O(7)−Rh(1)−N(2)	89(1)
O(4)−Rh(1)−N(1)	96(1)	N(1)−Rh(1)−N(2)	81(1)
O(4)−Rh(1)−N(2)	175(1)	O(1)−Rh(2)−N(4)	95(1)
O(3)−Rh(2)−O(5)	88(1)	O(5)−Rh(2)−N(3)	91(1)
O(3)−Rh(2)−N(3)	95(1)	O(5)−Rh(2)−N(4)	93(1)
O(3)−Rh(2)−N(4)	176(1)	N(3)−Rh(2)−N(4)	81(1)

(22) Le, J. C.; Chavan, M. Y.; Chau, L. K.; Bear, J. L.; Kadish, K. M. *J. Am. Chem. Soc.* **1985**, *107*, 7195.

(23) (a) Eastland, G. W.; Symons, M. C. R. *J. Chem. Soc., Dalton Trans.* **1984**, 2193. (b) Pruchnik, F.; Jezierski, A.; Kalecinska, E. *Polyhedron* **1991**, *10*, 2551.

(24) (a) Boyd, D. C.; Connelly, N. G.; Garcia Herbosa, G.; Hill, M. G.; Mann, K. R.; Mealli, C.; Orpen, A. G.; Richardson, K. E.; Rieger, P. H. *Inorg. Chem.* **1994**, *33*, 960. (b) Hill, M. G.; Mann, K. R. *Inorg. Chem.* **1991**, *30*, 1429. (c) Connelly, N. G.; Loyns, A. C.; Fernandez, M. J.; Modrego, J.; Oro, L. A. *J. Chem. Soc., Dalton Trans.* **1989**, 683. (d) Connelly, N. G.; Loyns, A. C. *J. Organomet. Chem.* **1991**, *411*, 285. (e) Brauns, T.; Carriedo, C.; Cockayne, J. A.; Connelly, N. G.; Garcia Herbosa, G.; Orpen, A. G. *J. Chem. Soc., Dalton Trans.* **1989**, 2049.

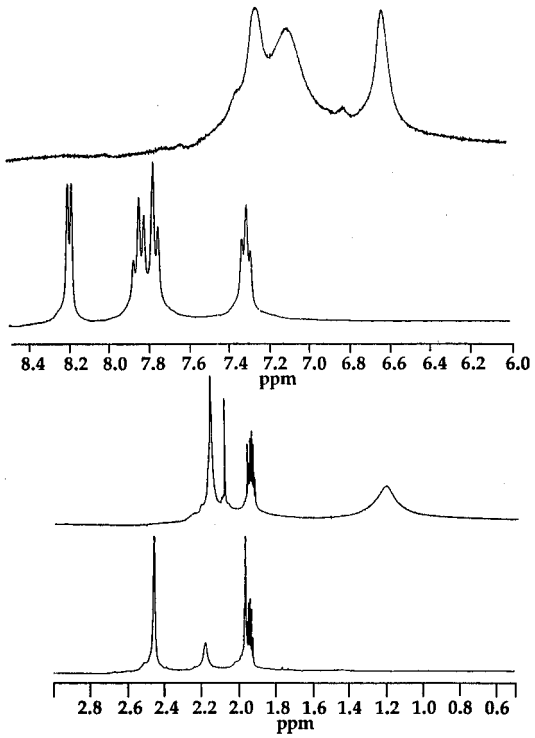

Figure 4. ^{1}H NMR spectra in CD_3CN at ~23 °C of complexes **14** (top) and **6b** (bottom).

Table 7. Selected Bond Distances (Å) and Angles (deg) for $[Rh_2(O_2CPh)(tpy)_2(MeCN)_2](BF_4)_3$·MeCN (**16**)

(a) Bonds

Rh(1)−Rh(2)	2.6286(10)	Rh(2)−O(5)	2.060(4)
Rh(1)−O(3)	2.074(4)	Rh(2)−N(33)	2.044(5)
Rh(1)−N(12)	2.050(5)	Rh(2)−N(44)	1.945(5)
Rh(1)−N(23)	1.931(5)	Rh(2)−N(50)	2.038(5)
Rh(1)−N(29)	2.043(5)	Rh(2)−N(51)	2.181(5)
Rh(1)−N(30)	2.154(5)		

(b) Angles

Rh(2)−Rh(1)−O(3)	82.83(11)	Rh(1)−Rh(2)−O(5)	83.10(11)
Rh(2)−Rh(1)−N(12)	93.82(13)	Rh(1)−Rh(2)−N(33)	92.47(14)
Rh(2)−Rh(1)−N(23)	95.80(14)	Rh(1)−Rh(2)−N(44)	96.83(14)
Rh(2)−Rh(1)−N(29)	92.54(13)	Rh(1)−Rh(2)−N(50)	94.25(13)
Rh(2)−Rh(1)−N(30)	170.39(14)	Rh(1)−Rh(2)−N(51)	171.94(14)
O(3)− Rh(1)−N(12)	100.87(19)	O(5)− Rh(2)−N(33)	98.80(21)
O(3)− Rh(1)−N(23)	177.97(18)	O(5)− Rh(2)−N(44)	179.62(19)
O(3)− Rh(1)−N(30)	87.70(17)	O(5)− Rh(2)−N(51)	88.98(18)
N(12)−Rh(1)−N(23)	80.69(22)	N(33)−Rh(2)−N(44)	80.83(22)
N(12)−Rh(1)−N(29)	160.70(21)	N(33)−Rh(2)−N(50)	161.06(21)
N(12)−Rh(1)−N(30)	89.56(19)	N(33)−Rh(2)−N(51)	87.29(20)
N(23)−Rh(1)−N(29)	80.55(21)	N(44)−Rh(2)−N(50)	80.80(20)
N(23)−Rh(1)−N(30)	93.62(19)	N(44)−Rh(2)−N(51)	91.08(19)

arises from the following electronic configuration involving Rh d-orbital overlap: $\sigma^2\pi^4\delta^2\delta^{*2}\pi^{*4}$. This leads to the standard, net Rh−Rh single bond description. A one-electron oxidation yields a $\sigma^2\pi^4\delta^2\delta^{*2}\pi^{*3}$ configuration and a resultant bond order of 1.5, whereas a one-electron reduction would involve population of the high-energy σ-antibonding orbital (assuming that it is the HOMO) to yield a $\sigma^2\pi^4\delta^2\delta^{*2}\pi^{*4}\sigma^{*1}$ configuration and a bond order of 0.5. It is thus intuitively acceptable that reversible oxidations of $[Rh_2]^{4+}$ complexes are relatively common whereas reversible reductions are not.[22] To discover that the $[Rh_2(O_2CR)_2(L\text{-}L)_2]^{2+}$ complexes support reversible reductions at relatively accessible potentials was therefore of some interest. Close examination of the data in Table 9, however, reveals some interesting points: (i) the variation of the potential of the reversible reduction as a function of the carboxylate is essentially insignificant within experimental error (±0.01 V); (ii) in contrast, altering the electronic character of the chelate, with the carboxylate kept constant (R = Me), causes dramatic changes to the reduction potential, from −0.89 V for L-L = bpy (**6**) to −0.61 V for L-L = Ph_2bpy (**12**), a range of 280 mV; and (iii) for the Ph_2bpy (**12**) and Ph_2phen (**13**) complexes, coulometry indicates the reduction to be a *two-electron* process, and addition of two electrons into the σ^* orbital would give a Rh−Rh bond order of 0 and effectively Rh^I monomers, a situation that might intuitively be expected to make the process appear less reversible by electrochemical criteria. As shown in Figure 6, however, the CV scan of **13** shows a reduction feature that retains the overall appearance of that in Figure 5, albeit with an increased Δp value (~300 mV) and an increased

Table 8. ^{1}H NMR Data[a] for Complexes **5**−**13** and **16**

				δ	
complex	solvent	R	chelate	RCO_2^-	chelate
5	CD_3OD	Me	bpy	1.90, 2.60	7.44, 7.95, 8.00, 8.38
6b	CD_3CN	Me	bpy	2.52	7.28, 7.71, 7.82, 8.16
7	CD_3CN	Et	bpy	1.32, 2.73	7.30, 7.73, 7.84, 8.13
8	CD_3CN	Ph	bpy	7.57, 7.68, 8.28	7.25, 7.77, 7.85, 8.21
9	CD_3CN	CF_3	bpy	na	7.23, 7.72, 7.81, 8.12
10	CD_3CN	Me	phen	2.57	7.54, 7.63, 8.18, 8.39
11	CD_3CN	Me	Me_2bpy	2.41	2.45 (Me), 7.14, 7.64, 7.94
12	CD_3CN	Me	Ph_2bpy	2.52	7.39, 7.48, 7.61, 8.17, 8.29
13	CD_3CN	Me	Ph_2phen	2.62	7.24, 7.45, 7.55, 7.60, 7.74, 8.55
16	CD_3CN	Ph	tpy	7.74, 7.85, 8.55	7.47, 7.59, 7.95, 8.06, 8.14, 8.17

[a] ~23 °C, na = not applicable. [b] Shifts are in ppm and referenced *vs* the protio impurity of the solvent employed.

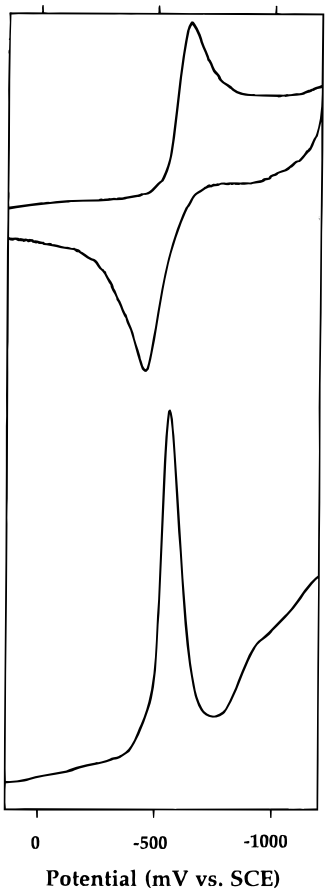

Figure 5. The cyclic voltammogram at 100 mV/s and differential pulse voltammogram at 5 mV/s of complex **6a** in MeCN containing NBu^n_4-PF_6.

Table 9. Electrochemical Data[a] for $[Rh_2(O_2CR)_2(N\text{-}N)_2]^{2+}$ Complexes in MeCN

complex	R	N-N	E_{red}	n^b	E_{ox}	n
6a	Me	bpy	−0.89	1		
7	Et	bpy	−0.91	1		
8	Ph	bpy	−0.87	1		
10	Me	phen	−0.83	1		
11	Me	Me_2-bpy	−0.95	1		
12	Me	Ph_2-bpy	−0.61	2	0.68	1
13	Me	Ph_2-phen	−0.76	2	0.89	1

[a] Potentials are volts vs ferrocene/ferrocenium; values were obtained from the DPV peaks and are estimated as ±0.01 V. [b] Electrons involved in the redox couple.

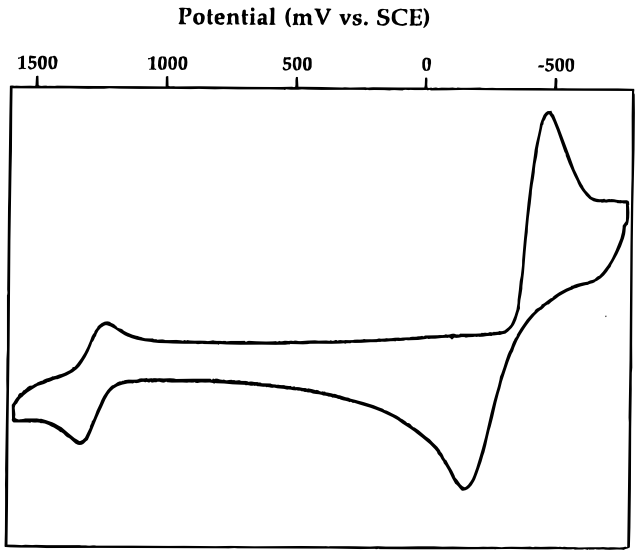

Figure 6. The cyclic voltammogram at 100 mV/s of complex **13** in MeCN containing $NBu^n_4PF_6$.

asymmetry between forward and reverse waves. The overall appearance does not change significantly at lower scan rates. Interestingly, **13** also exhibits a reversible, one-electron oxidation couple at +0.89 V assignable to the formation of the $[Rh_2]^{5+}$ species (i.e., $Rh^{II}Rh^{III}$). The conclusion suggested by observations i−iii is that the reductions are primarily ligand- rather than metal-based and do not therefore involve population of the Rh−Rh σ^* orbital. As such, the potentials should be more sensitive to changes in the nature of the electron-acceptor ligands rather than the ancillary ligands, i.e., to the chelating groups (bpy etc.) rather than the RCO_2^- groups. This conclusion is consistent with the results of EHT calculations by Pruchnik[3f] on $[Rh_2(O_2CH)_2(HN(CH)_2NH)_2X_2]$ ($HN(CH)_2NH$ = 1,4-diazabutadiene, X = Cl, Br) which showed the LUMO to be primarily ligand ($HN(CH)_2NH$) in character and allowed the prediction that reduction of $[Rh_2(O_2CR)_2(bpy)_2]^{2+}$ would be ligand-based. To complement this previous calculation and to probe the nature of the LUMO further, an EHT calculation has been carried out on a model complex possessing bpy rather than 1,4-diazabutadiene groups and neutral rather than halide axial ligands.

EHT Calculations. EHT calculations were performed on the model complex $[Rh_2(O_2CH)_2(bpy)_2(HCN)_2]^{2+}$ of C_{2v} symmetry. The results of the calculation are summarized in Figure 7. Note the axis-labeling scheme, which places the *z* axis along the Rh−Rh vector and the *x* and *y* axes bisecting the metal−ligand bonds.

In an idealized D_{4h} system, such as $Rh_2(O_2CH)_4(MeOH)_2$, the 14-electron $[Rh_2]^{4+}$ core has the configuration $\sigma^2\pi^4\delta^2\delta^{*2}\pi^{*4}$ with a net single bond owing to the high-energy σ^* orbital being unoccupied. A similar configuration is observed for $[Rh_2(O_2CH)_2(bpy)_2(HCN)_2]^{2+}$, as shown in Figure 7, with an energy

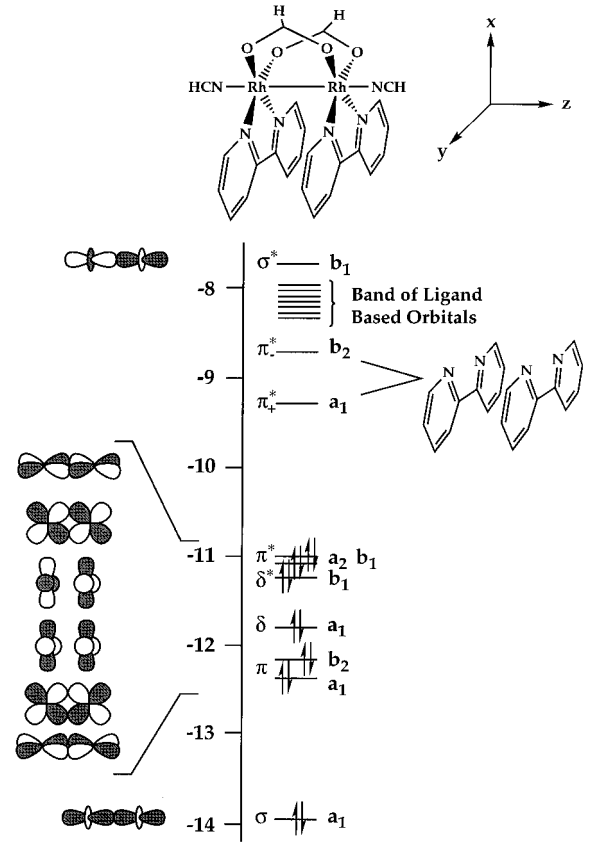

Figure 7. Molecular orbital energy diagram resulting from the EHT calculation on $[Rh_2(O_2CH)_2(bpy)_2(HCN)_2]^{2+}$.

splitting of both the two π and two π^* orbitals owing to the lower symmetry (C_{2v}) of the complex. The HOMO is thus a Rh−Rh π^* orbital of b_1 symmetry. However, the LUMO of $[Rh_2(O_2CH)_2(bpy)_2(HCN)_2]^{2+}$ is not the σ^* orbital of the $[Rh_2]^{4+}$ system. Between the HOMO and the σ^* orbital is a band of ligand-based orbitals, composed predominantly of the π^* orbitals of the bpy rings (henceforth referred to as bpy-π^* to distinguish between these and the $[Rh_2]^{4+}$ π^* orbitals). The most pertinent to our discussion are the lowest two orbitals in this band, which represent the LUMO and the second-lowest unoccupied orbital (SLUMO) of the molecule. Because the two bpy groups are coordinated *syn* about the dinuclear core, the two bpy π-systems are brought into close proximity and interact. As a result, the LUMO and SLUMO are, in fact, in-phase and out-of-phase combinations, respectively, of one of the bpy-π^* orbitals on each bpy group; these two combinations are designated $\pi^{\ddagger}$ (a_1) and $\pi^{\pm}$ (b_2) and are depicted in Figure 8. The in-phase ($\pi^{\ddagger}$) and out-of-phase ($\pi^{\pm}$) overlap is of σ symmetry and corresponds to a bonding and an antibonding interaction, respectively, between the two bpy groups, which lowers the energy of the $\pi^{\ddagger}$ and raises the energy of the $\pi^{\pm}$ orbitals relative to the isolated Rh(bpy) fragment; the resultant LUMO−SLUMO gap is 0.65 eV. Consideration of the atomic contributions to the molecular orbitals indicates that the HOMO of the complex is exclusively metal π^* in character (>98%) while the LUMO and SLUMO are predominantly bpy-based with only very small metal π character; the LUMO and SLUMO contain ∼7 and ∼9% metal character, respectively. Additionally, the band of ligand-based orbitals between the SLUMO of the complex and the metal−metal σ^* orbital is composed of 10 molecular orbitals based predominantly on the bpy ligands or the axial nitrile molecules.

The picture that emerges from the EHT calculation is a $[Rh_2(O_2CH)_2(bpy)_2(HCN)_2]^{2+}$ molecule with a HOMO that is Rh−Rh π^* in character and a LUMO that is predominantly

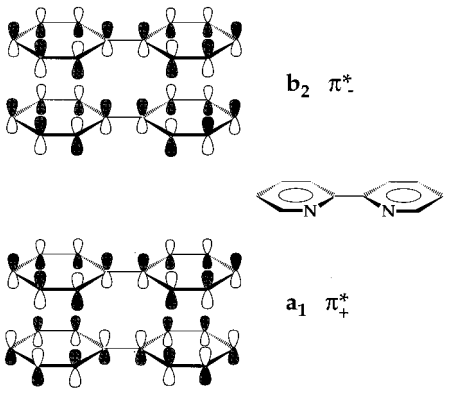

Figure 8. Depiction of the LUMO (π^*_+) and SLUMO (π^*_-) of $[Rh_2(O_2CH)_2(bpy)_2(HCN)_2]^{2+}$.

ligand (bpy)-based, with a HOMO−LUMO gap of 1.76 eV; the LUMO represents an inter-bpy bonding interaction. Oxidation of such a molecule would thus yield a species with a Rh−Rh bond order of 1.5 whereas reduction involves population of a $(bpy)_2$ bonding orbital with no change to the Rh−Rh bond order. Extrapolation of these conclusions back to the $[Rh_2(O_2CR)_2(L\text{-}L)_2]^{2+}$ complexes rationalizes the presence of a reversible reduction in the electrochemical studies whereas this is not observed in the parent $[Rh_2(O_2CR)_4(L)_2]$ complexes, which obviously contain no bpy.

It is interesting to note that the reversible reduction process seems to require the presence of two *syn*-bpy groups; not only is such a redox couple not observed in $[Rh_2(O_2CR)_4(L)_2]$ complexes, it is also not present in the mono-bpy complexes described elsewhere, namely, $[Rh_2(O_2CMe)_3(bpy)(MeOH)](O_2CMe)$ and $[Rh_2(O_2CMe)_2(bpy)(MeCN)_4](BF_4)_2$.[6b] These complexes also contain eq,eq-coordinated bpy groups but display no reversible reduction processes, within the accessible potential range of our experiments at least. Note also that the bridging $MeCO_2^-$ groups of $[Rh_2(O_2CMe)_2(bpy)_2]^{2+}$ can be removed[16] with a carboxylate-abstracting reagent to give $[Rh_2(bpy)_2(MeCN)_6]^{4+}$; the latter complex now shows no reversible reduction processes, which we consider to probably be due to the fact that free rotation about the Rh−Rh single bond is now possible and the bpy groups are therefore no longer locked into a *syn* conformation in solution, effectively destroying the stabilizing bpy−bpy overlap; i.e., the low-lying, inter-bpy π^*_+ orbital is no longer available.

An additional question that springs to mind is to what extent the inter-bpy bonding (π^*_+) and antibonding (π^*_-) interactions and the reversibility of the reduction process are affected by the eclipsed *vs* staggered possibilities for the two *syn*-bpy groups. In tetrabridged $Rh_2(O_2CR)_4L_2$ complexes, the staggered conformation is slightly preferred on steric grounds but the presence of four bridging RCO_2^- groups effectively locks in an eclipsed conformation (torsional angles typically <3°). In the $[Rh_2(O_2CR)_2(N\text{-}N)_2]^{2+}$ complexes, the two remaining RCO_2^- groups appear sufficient to maintain an essentially eclipsed conformation in the solid state (torsional angle of ∼6° in **6a**). In the cation of complex **16**, $[Rh_2(O_2CPh)(tpy)_2(MeCN)_2]^{3+}$, there is only one bridging ligand and the average torsion angle is now a much larger 21.6° in the solid state. Although the solution ^1H NMR spectrum indicates effective C_{2v} symmetry in solution consistent with a dynamic process involving rotational oscillation about the Rh−Rh bond *via* the eclipsed conformation, the amplitude of this oscillation would be large and the solution form would not approximate to eclipsed. It is thus consistent with the earlier discussion to note that complex **16** shows no reversible reduction, in stark contrast to the $[Rh_2(O_2CR)_2(N\text{-}N)_2]^{2+}$ complexes.

In the case of the tpy-containing complex $[Rh_2(O_2CH)(tpy)_2(HCN)_2]^{3+}$, EHT calculations again show a HOMO of essentially pure metal π^*. Analogous with the bpy system, the LUMO is again inter-tpy σ in character, with equal contributions from both tpy ligands to the molecular orbital, involving in-phase overlap of a π^* orbital on each tpy group; again, the SLUMO is the out-of-phase counterpart of this π-stacking orbital. However, due to the large torsion angle and relatively staggered conformation within the tpy complex, the overlap between the two π -systems is much smaller than in the bpy case, and this results in a very small LUMO−SLUMO gap of only 0.10 eV. This therefore produces a system where the π^* orbitals of the tpy ligands are minimally stabilized relative to the free ligand, in marked contrast to the bpy system where the eclipsed conformation enforces significant π overlap and resultant stabilization.

Generation and Isolation of Reduced Species. The coulometry experiment at −0.99 V on complex **6b** in MeCN confirmed the one-electron nature of the reduction and gave an intense blue color that displayed long-term stability under an inert atmosphere. This stimulated attempts to isolate the reduced material. Following exhaustive electrolysis of a 0.1 mM solution of **6b** in MeCN at −0.99 V with $NBu^n_4PF_6$ as the supporting electrolyte, the dark blue solution was transferred to a Schlenk flask and treated with Et_2O to precipitate a dark blue solid. For larger scale generation of the reduced material, an orange-red MeCN solution of **6b** was treated with a slight molar excess of Na acenaphthylenide and Et_2O added to the dark blue solution to give a dark blue solid in 72% yield. Recrystallization from MeCN/Et_2O gave thin blue needles that were unfortunately not suitable for crystallographic studies. Numerous attempts to grow suitable crystals proved unsuccessful. The same procedure was employed for the preparation of the PF_6^-, SbF_6^-, $CF_3SO_3^-$, and $W_6O_{19}^{2-}$ salts, among others, but in no case were suitable crystals obtained. This was unfortunate, because the EHT calculation predicts the LUMO to be ligand-based and bpy/bpy-bonding in nature (*vide supra*), suggesting that the Rh−Rh bond in **14** might be very similar to that in **6a** and that the bpy rings might be slightly closer together, which would presumably mean that the splaying apart of the bpy groups seen in **6a** would not be as great in **14**. Such a small but significant structural change could be the origin of the CV behavior being less-than-ideal *vis-à-vis* electrochemical criteria for a reversible reduction. Further, the coulometric identification of the reduction of $[Rh_2(O_2CMe)_2(Ph_2phen)_2]^{2+}$ (**13**) as being a two-electron process and the large LUMO−SLUMO gap in the EHT calculation on $[Rh_2(O_2CH)_2(bpy)_2(HCN)_2]^{2+}$ suggest that the two added electrons both go into the LUMO, no doubt facilitated by the more extensive π-system in Ph_2phen *vs* bpy or phen, which can thus better accommodate two electrons. The greater structural consequences of two-electron reduction could also explain the Δp and shape differences in the CV's of **6b** *vs* **13** (Figures 5 and 6, respectively). Further considerations of the structural consequences of one- or two-electron reduction must, however, await additional attempts to structurally characterize **6** (or a related complex) and new attempts to similarly characterize doubly-reduced **12** or **13**.

The ^1H NMR spectrum of **14** in CD_3CN is shown in Figure 4, where it can be compared with that of **6**. The increased line widths, loss of resolution of spin−spin coupling, and small changes in chemical shifts are consistent with a paramagnetic species. The overall appearance of the spectrum is consistent with retention of the effective C_{2v} solution symmetry of **6** on reduction. The $S = {}^1/_2$ nature of the cation of **14** was confirmed

by an Evans determination in MeCN solution of the effective magnetic moment ($\mu_{eff} = 2.05\ \mu_B$). An EPR spectrum of an MeCN solution displayed only a very broad featureless signal in the $g \approx 2$ region which looked very unlike the axial or rhombic spectra displaying Rh hyperfine structure normally observed for oxidized $[Rh_2]^{5+}$ or reduced $[Rh_2]^{3+}$ species where the unpaired electron is metal-based.[2h,22−24] Similarly broad signals have been reported, however, for mononuclear Pt^{II} complexes that possess bpy or phen groups and are reduced by one electron, the reduction being primarily ligand-based with only a few percent metal character.[25] The spectrum of **14** appears to be most similar, in fact, to the one-electron-reduced version of $[Pt(bpy)(MebpyH)]^{2+}$ (Mebpy-H = *N*-methyl-2,2′-bipyridinyl-*C(3),N*′), which shows a broad, featureless signal at $g \approx 2$ and which the authors suggest might be due to the unpaired electron being delocalized over both the bpy and MebpyH groups. This would be analogous to the situation in **14**.

The electronic spectrum of **14** in MeCN is shown in Figure 9, which also contains the spectrum of **6b** for comparison. Intense absorption bands in the visible region are evident and are assigned to bpy−bpy transitions from the singly-occupied MO (SOMO) of **14** to empty bpy π^* orbitals that represent the LUMO and other low-lying empty orbitals. That the bands are not due to MLCT transitions is supported by the essentially unchanged electronic spectral features in a variety of solvents of various polarities and the absence of corresponding bands in the spectrum of **6**. Appearance of intense absorption bands in the visible region is also observed on the primarily ligand-based reductions of the $[Pt(bpy)(py)_2]^{2+}$ and related complexes mentioned above,[25] the new absorption bands being assigned to intraligand π-to-π^* and π^*-to-π^* transitions of coordinated bpy^-.

Complexes **5** and **6** can also be reduced by heating alcohol solutions to ∼80 °C; heating an orange-red EtOH or Pr^nOH solution under nitrogen leads to the appearance of a dark blue color, which persists on cooling of the solution to room temperature. The electronic spectrum of the dark blue solution is identical to that of isolated **14**, confirming the product in EtOH as being the one-electron-reduced species. Exposure of the cooled blue solution to air causes regeneration of the orange-red color. The use of alcohols to reduce **5** or **6** is reminiscent of the preparative procedure for the parent complex $Rh_2(OAc)_4(MeOH)_2$ (**1**), which is prepared by reduction of $RhCl_3 \cdot xH_2O$ in refluxing EtOH containing NaOAc and acetic acid, followed by removal of EtOH and crystallization from MeOH. Clearly, under these conditions the reduction stops at the Rh^{II}_2 level; in $[Rh_2(OAc)_2(bpy)_2(MeCN)_2]^{2+}$, the incorporation of two *syn*-bpy groups and its provision of a relatively low-lying bpy-based LUMO obviously make possible the donation by EtOH of an additional reducing equivalent to the Rh^{II}_2 system.

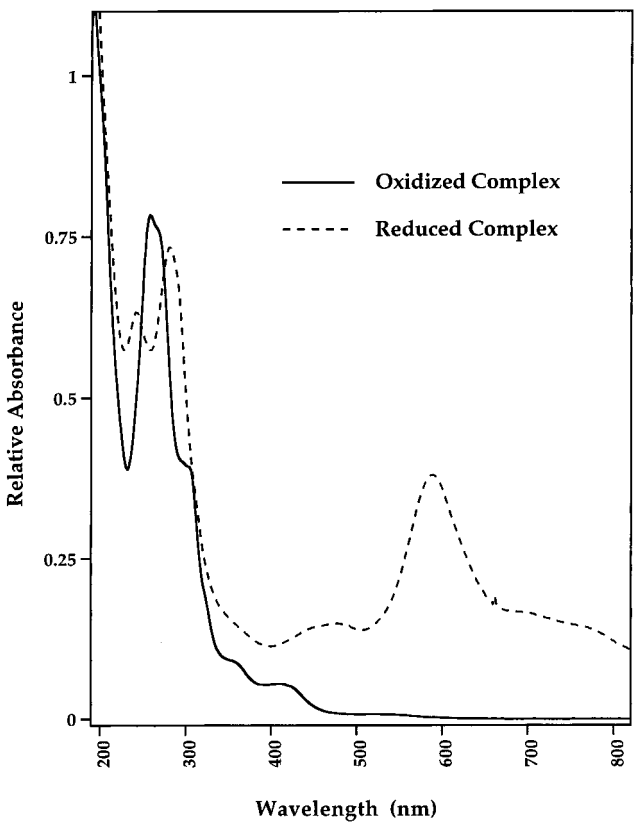

Figure 9. Electronic spectra of complexes **6** (—) and **14** (− − −) in MeCN.

Acknowledgment. This work was funded by NSF Grants CHE 9311904 (G.C.) and CHE 9311812 (K.R.D.). We thank Proctor and Gamble for a Fellowship to C.A.C.

Supporting Information Available: Tables of fractional coordinates, isotropic and anisotropic thermal parameters, fully labeled figures, and bond distances and angles for complexes **6a**, **9**, and **16** (41 pages). Ordering information is given on any current masthead page.

IC9610288

(25) Braterman, P. S.; Song, J.-I.; Wimmer, F. M.; Wimmer, S.; Kaim, W.; Klein, A.; Peacock, R. D. *Inorg. Chem.* **1992**, *31*, 5084.